THE JOURNAL OF BIOLOGICAL CHEMISTRY
Vol. 277, No. 45, Issue of November 8, pp. 42456–42462, 2002
Printed in U.S.A.

Intrinsically Slow Dynamic Instability of HeLa Cell Microtubules *in Vitro**

Received for publication, July 16, 2002, and in revised form, August 27, 2002
Published, JBC Papers in Press, August 30, 2002, DOI 10.1074/jbc.M207134200

Cori N. Newton‡§, Jennifer G. DeLuca¶, Richard H. Himes‖, Herbert P. Miller‡, Mary Ann Jordan‡, and Leslie Wilson‡

From the ‡Department of Molecular, Cellular, and Developmental Biology, University of California, Santa Barbara, California 93106 and the ‖Department of Molecular Biosciences, University of Kansas, Lawrence, Kansas 66045

The dynamic behavior of mammalian microtubules has been extensively studied, both in living cells and with microtubules assembled from purified brain tubulin. To understand the intrinsic dynamic behavior of mammalian nonneural microtubules, we purified tubulin from cultured HeLa cells. We find that HeLa cell microtubules exhibit remarkably slow dynamic instability, spending most of their time in an attenuated state. The tempered dynamics contrast sharply with the dynamics of microtubules prepared from purified bovine brain tubulin under similar conditions. In accord with their minimal dynamic instability, assembled HeLa cell microtubules displayed a slow treadmilling rate and a low guanosine-5′-triphosphate hydrolysis rate at steady state. We find that unlike brain tubulin, which consists of a heterogeneous mixture of β-tubulin isotypes (β_{II}, β_{III}, and β_{IV} and a low level of β_I), HeLa cell tubulin consists of β_I tubulin (~80%) and a minor amount of β_{IV} tubulin (~20%). The slow dynamic behavior of HeLa cell microtubules *in vitro* differs strikingly from the dynamic behavior of microtubules in living cultured mammalian cells, supporting the idea that accessory factors create the robust dynamics that occur in cells.

Microtubules are dynamic polymers that have important roles in many eukaryotic cell processes including the development and maintenance of cell shape and polarity, vesicular transport, and chromosome movements during mitosis and meiosis (reviewed in Refs. 1 and 2). Many of the cellular functions of microtubules rely on their unusual nonequilibrium polymerization dynamics, which facilitate the ability of the microtubules to change their organization rapidly to accommodate the needs of the cell. One such behavior is dynamic instability, a process in which microtubule ends switch between periods of growth, shortening (also called shrinking), and attenuation (3–5). Another dynamic behavior, which occurs at or near polymer mass steady state, is treadmilling, which involves net growth at the microtubule plus ends and equivalent shortening at the minus ends (6–9). Extensive studies have described the dynamic instability behavior of microtubules, both in living cells (10–13) and in cell-free purified systems (3–5).

Most studies on the dynamic instability behavior of microtubules *in vitro* have been carried out with tubulin purified from mammalian brain tissue (3–5, 14). Such neural microtubules, when assembled in the absence of microtubule-associated proteins (MAPs),[1] undergo growth and shortening dynamics that are qualitatively similar to the dynamic instability behavior displayed by many microtubules in cells. Despite the qualitative similarity, the dynamic instability behavior of neural microtubules *in vitro* differs quantitatively from that displayed by microtubules in cultured mammalian cells (10–13). The rates of growth and shortening and especially the switching frequencies among the growing, shortening, and attenuated states are considerably slower for brain microtubules *in vitro* than with those displayed by microtubules in cultured mammalian cells (reviewed in Refs. 2 and 15). For example, microtubules in cultured pig kidney LLCPK-1α cells grow at about 10-fold higher rates and they exhibit a considerably higher frequency of switching from the growing or attenuated state to rapid shortening (called the catastrophe frequency) than purified brain microtubules (13). Similarly, the treadmilling rates of brain microtubules *in vitro* are considerably lower than those observed in cells (7, 9). The intrinsic dynamic instability of microtubules *in vitro* from sources other than mammalian brain also appear to be reduced *in vitro* as compared with their dynamics in cells. These include microtubules assembled from purified sea urchin egg tubulin (*Strongylocentrotus purpuratus*) and yeast (*Saccharomyces cerevisiae*) tubulin (16–18).

Several possibilities could account for the reduced dynamics of microtubules made from nonneural mammalian tubulin *in vitro*. One is that the solution conditions used in the *in vitro* experiments are not optimal for obtaining rapid dynamics. However, Simon *et al.* (16) studied the influence of solution conditions on the dynamic instability of sea urchin microtubules *in vitro* and concluded that the ambient ionic conditions of the cytoplasm could not account for the fast elongation rates or high catastrophe frequencies of microtubules found in living cells. Another possibility is that the more rapid dynamics of microtubules displayed in cells as compared with microtubules *in vitro* is because of cellular factors that increase the dynamics of the microtubules (*e.g.* catastrophe factors, Refs. 2, 15, and 19–22). This is an attractive possibility that appears to occur in yeast. Differences in tubulins cannot easily explain why microtubules in yeast cells are much more dynamic than those formed from purified yeast tubulin (18).

* This work was supported in part by United States Public Health Service Grants NS13560 and CA57291, University of California Biotechnology Research and Teaching Program Grant 99-14, and the Materials Research Laboratory Program of the National Science Foundation under Award DMR00-80034. The costs of publication of this article were defrayed in part by the payment of page charges. This article must therefore be hereby marked "*advertisement*" in accordance with 18 U.S.C. Section 1734 solely to indicate this fact.

§ To whom correspondence should be addressed. E-mail: newton@lifesci.ucsb.edu.

¶ Current address: Dept. of Biology, University of North Carolina, Chapel Hill, NC 27599.

[1] The abbreviations used are: MAPs, microtubule-associated proteins; PIPES, 1,4-piperazinediethanesulfonic acid; DTT, dithiothreitol; HSS, high speed supernatant; MES, 2-(*N*-morpholino)ethanesulfonic acid.

While microtubule dynamic instability has been well studied in living mammalian-cultured cells, the dynamic properties of microtubules composed solely of purified tubulin from such cells have not been analyzed. To determine the intrinsic dynamics behavior of microtubules assembled from nonneural mammalian cell tubulin, we characterized the dynamic properties of microtubules assembled from highly purified HeLa cell tubulin. We find that these microtubules display remarkably limited dynamic instability and treadmilling behaviors when compared with those of brain microtubules analyzed under identical conditions *in vitro*. These data support the hypothesis that the rapid dynamics of the microtubules observed in such cells are caused by nontubulin regulatory factors.

EXPERIMENTAL PROCEDURES

Purification of HeLa Cell Tubulin—HeLa cells were grown in 20-liter carboys on magnetic stir plates at 37 °C in medium containing 50% Dulbecco's modified Eagle's medium and 50% F-12 medium supplemented with HEPES, glucose, $NaHCO_3$, modified Eagle's medium nonessential amino acids, penicillin, streptomycin, and 2% iron-supplemented calf serum (23). Cells were collected from 40–70-liter suspensions of exponentially growing cultures at a density of $\sim 10^6$ cells/ml by centrifugation at 8000 rpm with a continuous flow rotor adapter system as previously described (23). The collected cells were washed once by resuspension in a buffer consisting of 50 mM PIPES, 1 mM EGTA, 1 mM magnesium sulfate, 0.05% sodium azide, pH 6.9 (PEM50), and sedimented in a tabletop clinical microcentrifuge (3000 *x g*). The pellet was resuspended at a 1:1 ratio (v/v) of packed cells to PEM50 containing 1 mM DTT and a mixture of protease inhibitors (2.5 μM 4-(2-aminoethyl)benzenesulfonyl fluoride, 1 μg/ml pepstatin A, 1 μg/ml leupeptin, 1 mM tosylarginine methyl ester, and 10 μg/ml aprotinin) (PEM50DP). The cells were then frozen dropwise in liquid nitrogen and stored as long as 4 months at −70 °C.

Tubulin was purified from the HeLa cells by a protocol modified from Sackett (24). Approximately 70 ml of packed frozen cells were thawed and lysed by pulse sonication (Branson sonifier 450, Branson Ultrasonics Corp., Danbury, CT) at low energy (20 watts) on ice. The cell lysate was incubated on ice for 30 min to depolymerize the microtubules. A clarified high speed supernatant (HSS) was prepared by centrifugation of the lysate at 100,000 × *g* for 1 h at 4 °C. The HSS (~50–100 ml, 1.5–2 g of total protein) was batch-absorbed to hydrated DEAE-cellulose (DE52, Whatman) at a ratio of 44 mg of HSS protein to 1 ml of packed DEAE-cellulose for 30 min at 4 °C on a tabletop rocker. The slurry was poured into a 2.5 × 50-cm column and the flow-through fraction was discarded. The column was washed with 125 ml of PEM50DP and the flow-through fraction was also discarded. The column was then washed with 125 ml of PEM100 (100 mM PIPES, 1 mM EGTA, 1 mM $MgSO_4$, 1 mM DTT, 0.05% sodium azide, pH 6.9) and protease inhibitors (the same composition as in PEM50DP) containing 0.2 M sodium glutamate (0.2 M sodium glutamate/PEM100 buffer). The flow-through, which was discarded, contained weakly adsorbed contaminating proteins. Tubulin and other bound proteins were then eluted and collected in 4-ml fractions with 1 M sodium glutamate/PEM100 buffer. Fractions containing 0.6 mg/ml protein or more were pooled, GTP was added to a final concentration of 1 mM and the solution was incubated for 30 min at 35 °C to polymerize the tubulin. The resulting microtubules were sedimented by centrifugation in a Beckman L5-50 ultracentrifuge (60 Ti rotor, 35 °C, 50,000 × *g*, 45 min). The collected microtubules were then resuspended in 1–2 ml of PEM100 buffer and depolymerized on ice for 30 min with occasional homogenization (approximately every 5 min) with a Dounce homogenizer. The suspension was clarified by centrifugation in a Sorvall 5B Plus Super Speed centrifuge (SS-34 rotor, 4 °C, 18,000 rpm, 10 min). The clarified supernatant was frozen dropwise in liquid nitrogen and stored at −70 °C. No contaminating nontubulin proteins were detected in the final microtubule pellet, as evaluated by SDS-polyacrylamide gel electrophoresis and staining with Coomassie Blue.

Purification of Microtubule Protein from Bovine Brain—Bovine brain microtubule protein (70–80% tubulin, 20–30% MAPs) and purified bovine brain tubulin were isolated and stored as frozen drops in liquid nitrogen as previously described (9).

Protein Determination—Protein concentrations were determined by the Bradford method using bovine serum albumin as the standard (25).

Determination of the Critical Tubulin Concentration—HeLa cell tubulin at various total protein concentrations in PEM100 buffer containing 1 mM GTP and 1 mM DTT was incubated at 35 °C for 45 min. The microtubules were separated from soluble tubulin by centrifugation at 50,000 rpm in a Beckman Optima MAX ultracentrifuge (TLA, 100.3 rotor) for 45 min. Supernatants were removed and the protein concentrations were determined. The polymer mass at each protein concentration was determined by subtracting the tubulin concentration remaining in the supernatant from the total starting protein concentration. The steady-state critical concentration was determined as described by Detrich and Wilson (26).

Analysis of the Dynamic Instability of HeLa Cell and Bovine Brain Microtubules by Video Microscopy—Highly purified HeLa cell tubulin (7.7 μM), or bovine brain tubulin (14 μM) was mixed with axonemal seeds prepared from *Strongylocentrotus purpuratus* sperm in a buffer consisting of 87 mM PIPES, 36 mM MES, 1.4 mM $MgCl_2$, 1 mM EGTA, 1 mM DTT, and 1 mM GTP, pH 6.9 (PMEM buffer). Tubulin was polymerized for 30 min at 35 °C to reach steady state prior to analysis. For video microscopy, 2-μl samples were applied to glass microscope slides and placed on a preheated (35 °C) microscope stage. The dynamic instability behavior of the microtubules was imaged by video-enhanced differential interference contrast microscopy using a Zeiss IM35 inverted microscope with a 63× (1.4 numerical aperture) oil immersion objective. Growth of the brain microtubules occurred at both the plus and minus ends of the axonemes. The plus ends of brain microtubules were distinguished from the minus ends by their higher growth rates, greater excursion lengths, and larger number of microtubules per axoneme end as previously reported (5, 27). In contrast, HeLa cell microtubule growth occurred predominantly at one end of the seeds. Because of the long lengths of the microtubules at one end, and the small number of short microtubules that formed at the opposite ends of the seeds, we assumed that the long microtubules had grown from the plus ends of the seeds. Samples on the slides were recorded for a maximum of 35 min, and individual microtubules were recorded and analyzed between 2 and 10 min.

Microtubule images were captured in real-time and recorded on super VHS videotape. The microtubule lengths were measured every 3 s and analyzed using the Real Time Measurement program (Neal Gliksman and E. D. Salmon, University of North Carolina, Chapel Hill, NC). Growth and shortening events were determined by least squares regression of life history plots of microtubule length *versus* time. A microtubule was considered to be in a growth phase if the increase in length was greater than 0.2 μm at a rate greater than 0.10 μm/min. A microtubule was considered to be in a shortening phase when its shortening rate was >0.30 μm/min and its length changed by >0.2 μm. A microtubule was considered to be in an attenuated (paused) state when the change in length was ≤0.2 μm with a duration >30 s.

Determination of Treadmilling Rates—The treadmilling rates of HeLa cell microtubules and MAP-rich bovine brain microtubules were determined at polymer mass steady state by measuring the rate of [^{3}H]GTP incorporation into the polymers. HeLa cell tubulin and bovine brain microtubule protein (35 μM) were polymerized at 35 °C for 30 min in PEM100 buffer containing 0.1 mM GTP, 1 mM DTT, and a GTP regenerating system (1 unit/ml acetate kinase and 10 mM acetylphosphate). At steady state, the suspension was divided into 125-μl aliquots in 1.5-ml microtubes for the individual pulse time points and incubated for an additional 15 min to re-establish steady state. Each sample was pulsed with 5 μl of [^{3}H]GTP, begining with the 60-min time sample, followed at the appropriate time with the 30-, 20-, and 10- min samples. At the end of the total 60-min pulse, all samples were centrifuged simultaneously for 60 min at 35,000 rpm (35 °C) in a Beckman Optima MAX ultracentrifuge (TLA 100.3 rotor) to collect the microtubule pellets. An aliquot (50 μl) of each supernatant was removed to determine the specific activity of the [^{3}H]GTP. Pellets were gently washed with 1 ml of 30% sucrose in PEM100 buffer, resuspended in the PEM100 buffer, and incubated on ice at 0 °C overnight to disassemble the microtubules. The protein concentration and the amount of [^{3}H]GTP incorporation were determined for each microtubule pellet. To determine the incorporation rate per microtubule, samples were removed prior to pulsing to determine the mean microtubule length by electron microscopy as described below. Background levels of [^{3}H]GTP were determined in tubulin samples incubated at 0 °C in the presence of 10 μM podophyllotoxin to prevent any microtubule polymerization. The treadmilling rate was determined by linear regression analysis of the incorporation data.

Determination of the Steady-state GTP Hydrolysis Rate—The rate of GTP hydrolysis per microtubule at steady state was determined using a malachite green assay (29) as described by Panda *et al.* (14). HeLa cell and brain tubulin (35 μM) were polymerized separately at 35 °C in PMEM buffer containing 1 mM GTP. At the appropriate times following establishment of steady state (30–60 min), samples were removed and

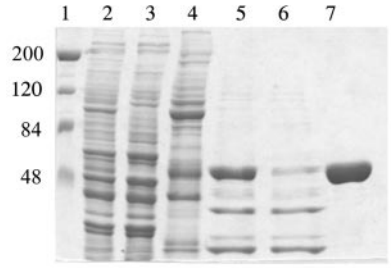

FIG. 1. **Purification of HeLa cell tubulin by column chromatography and microtubule assembly and disassembly.** A Coomassie Blue-stained SDS-PAGE gel shows the purification steps. *Lane 1*, molecular mass standards (kilodaltons); *lane 2*, clarified HSS; *lane 3*, initial DE-52 column flow-through; *lane 4*, 0.2 M sodium glutamate/PEM100 eluate; *lane 5*, 1 M sodium glutamate/PEM100 eluate; *lane 6*, warm supernatant after removal of the assembled microtubules; *lane 7*, 15 μg of purified HeLa cell tubulin after one cycle of assembly and disassembly.

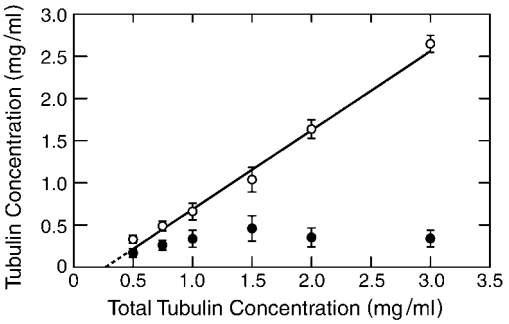

FIG. 2. **Critical concentration of purified HeLa cell microtubules.** HeLa cell tubulin was incubated for 45 min at 35 °C at the indicated initial total concentrations in PEM100 plus 1 mM GTP. Microtubule polymer was separated from soluble tubulin dimer by centrifugation and the protein concentrations in the supernatants were determined. The polymer concentrations (*open circles*) were determined by subtracting the supernatant concentration (*closed circles*) at each total tubulin concentration analyzed from the initial tubulin concentration. The average critical concentration was 0.3 mg/ml, as determined by extrapolation of the *x* intercept of the linear regression of polymer mass (three independent experiments).

added to 70% perchloric acid to achieve a final perchloric acid concentration of 7%. Samples were then incubated on ice for 20 min after which precipitated protein was sedimented by centrifugation for 4 min in a tabletop Biofuge A centrifuge. The supernatants were removed and aliquots were added to a solution of malachite green/ammonium molybdate. After 1 min, sodium citrate was added (final concentration of 10.2%) and the absorbance at 650 nm was measured after an additional 30 min. To determine the microtubule polymer mass, 100 μl of a polymerization reaction was centrifuged in a Beckman Optima MAX ultracentrifuge (50,000 rpm, 35 °C, 40 min). The supernatants were collected and protein concentrations were determined. The polymer mass was calculated by subtracting the supernatant concentration from the starting protein concentration.

Microtubule mean lengths and number concentrations were determined by electron microscopy (14). Briefly, samples of the microtubule suspensions were diluted into 0.2% glutaraldehyde, applied to grids, stained with 1% uranyl acetate, and viewed with a Jeol JEM-1230 electron microscope at ×2000 magnification. Mean microtubule lengths were determined with a Zeiss MOPIII program (more than 100 microtubules/sample were measured). The microtubule number concentration was then calculated from the mean length of the microtubules, the polymer mass, and a value of 1690 tubulin dimers/μm of microtubule length (14).

Determination of the β-Tubulin Isotype Composition—The β-tubulin isotype composition was determined both for tubulin in the clarified HeLa cell extracts and for the purified protein. Samples of HeLa cell clarified extracts and purified HeLa cell tubulin were analyzed by SDS-polyacrylamide gel electrophoresis and immunoblotting with specific β-tubulin monoclonal antibodies (β_I, β_{II}, β_{III}, and β_{IV}; generously provided by Dr. Richard Luduena, University of Texas Health Science Center, San Antonio, TX). Densitometric analysis was used to evaluate differences in protein levels of the samples (Alpha Imager program, Alpha Innotech Corp., San Leandro, CA).

RESULTS

Purification and Characterization of HeLa Cell Tubulin—To characterize the steady-state dynamic behavior of HeLa cell microtubules *in vitro*, milligram quantities of tubulin in a highly purified form had to be prepared. This was accomplished by growing large volumes of HeLa cells in suspension (23) and using a protocol modified from that described by Sackett (24) to purify the tubulin (see "Experimental Procedures"). Packed cells obtained from 70 liters of HeLa cell suspension were quick frozen in liquid nitrogen, thawed, lysed, and a HSS fraction was prepared (Fig. 1, *lane 2*). A slurry of DEAE-cellulose was added to the HSS and packed into a column, after which the column was washed (Fig. 1, *lanes 3* and *4*). Tubulin was eluted from the resin with 1.0 M sodium glutamate/PEM100 buffer (Fig. 1, *lane 5*). Tubulin was further purified to homogeneity by a single cycle of warm assembly-cold disassembly (Fig. 1, *lane 7*). All detectable contaminating proteins remained in the warm supernatant and none were detected in the tubulin fraction (Fig. 1, *lane 6*). The highly purified HeLa cell tubulin polymerized efficiently at 35 °C with a low critical subunit concentration as shown in Fig. 2. The critical concentration of the HeLa cell tubulin was 0.3 mg/ml (mean of three experiments). This value is comparable with the value of 0.5 mg/ml previously reported in a HeLa cell extract (30).

Steady-state Dynamic Instability at Plus Ends of HeLa Cell Microtubules—One of our goals was to analyze the steady-state dynamic instability of highly purified HeLa cell microtubules and to compare the behavior with that of purified brain microtubules. The plus end dynamics of individual HeLa cell microtubules were examined at steady state (35 °C) by video-enhanced DIC microscopy (see "Experimental Procedures") using PMEM buffer, a buffer previously used for analysis of brain microtubule dynamics (27, 31). Several life-history traces showing the changes in length of HeLa cell microtubules with time are shown in Fig. 3. The HeLa cell microtubules exhibited minimal dynamic instability. It is clear that they grew very slowly, rarely transitioned to rapid shortening, and spent a majority of the time in an attenuated (paused) state. In contrast, and similar to previous studies with bovine brain microtubules (27, 31), purified bovine brain microtubules displayed robust growing and shortening dynamics (Fig. 3).

The individual dynamic instability parameters determined from life-history plots both of HeLa cell microtubules and bovine brain microtubules are shown in Table I. When HeLa cell microtubules did grow, their growth rate was slow (0.2 μm/min), 33% of the rate of bovine brain microtubules. When HeLa cell microtubules shortened, their shortening rate was also very slow (7.8 μm/min), ~40% of the shortening rate of brain microtubules. The HeLa cell microtubules spent only 15% of their total time growing or shortening. In comparison, bovine brain microtubules spent 72% of their total time growing or shortening. In addition, the catastrophe frequency of HeLa cell microtubules was exceedingly low, with only 5 transitions to shortening observed for the 29 microtubules analyzed (172 min of total time analyzed). The catastrophe frequency (number of transitions per min of total time the microtubules spent growing and in the attenuated state) was only 0.02 events/min, a value only 13% of that for bovine brain microtubules. In contrast to bovine brain microtubules, every shortening event observed for HeLa cell microtubules was rescued, and the rescue frequency of HeLa cell microtubules was 3.7-fold higher than that of bovine brain microtubules. The dynamicity of HeLa cell microtubules (total detectable tubulin dimer exchange expressed in terms of μm/min) was only 4% that of brain micro-

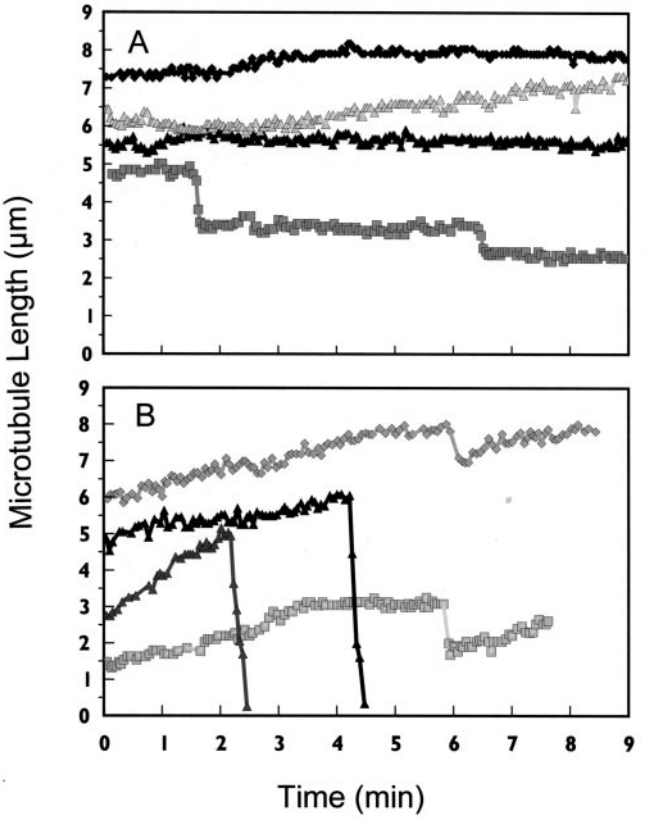

FIG. 3. **Life-history traces of microtubules at their plus ends.** *Panel A*, HeLa cell microtubules; *panel B*, bovine brain microtubules. Growing and shortening length changes for a number of individual axoneme-seeded HeLa cell (7.7 μM tubulin) and bovine brain (14 μM tubulin) microtubules are shown.

tubules. Thus, it is clear that HeLa cell microtubules *in vitro* exhibit minimal dynamic instability as compared with brain microtubules *in vitro*. Moreover, their dynamics are highly attenuated as compared with the dynamics of microtubules in living cultured mammalian cells (10–13).

Steady-state Treadmilling Rate of HeLa Cell Microtubules—In an effort to further understand the dynamic properties of purified HeLa microtubules we also evaluated their treadmilling behavior. The treadmilling behavior of HeLa cell microtubules was determined by pulsing the microtubules at steady state with [^{3}H]GTP. The linear incorporation of [^{3}H]GTP into HeLa cell microtubules in a typical experiment is shown in Fig. 4. In this experiment the treadmilling rate was 167 dimers/microtubule/min or 5.93 μm/h. The mean rate for three replicate experiments was 148 dimers/microtubule/min (5.26 $\pm$ 1.58 μm/h). The treadmilling rate of the MAP-free HeLa cell microtubules was only 2.1-fold faster than that of MAP-rich bovine brain microtubules (2.49 $\pm$ 1.03 μm/h), which treadmill extremely slowly because of their high MAP content (9). These data further illustrate the limited dynamic behavior of the purified HeLa cell microtubules.

Steady-state GTP Hydrolysis Rate of HeLa Cell Microtubules—The rate of GTP hydrolysis at steady state in a microtubule suspension is an indication of the amount of dynamic behavior occurring at the ends of the microtubules. Relatively nondynamic microtubules would be expected to have a low GTP hydrolysis rate, whereas dynamic microtubules would be expected to have a high GTP hydrolysis rate. Thus, we measured the steady-state rate of GTP hydrolysis of the HeLa cell microtubules. The cumulative number of orthophosphate (P_i) molecules released with time per microtubule is plotted for a typical experiment in Fig. 5. The hydrolysis rate per microtubule determined for the experiment shown in Fig. 5 was 1610 molecules of P_i per microtubule per min. This rate was only ~13% that of MAP-free bovine brain microtubules under the same conditions (Fig. 5, 12,800 molecules of P_i per microtubule per min). The mean GTP hydrolysis rate of the HeLa cell microtubules was 1390 $\pm$ 340 molecules of P_i per microtubule per min from four replicate experiments and for brain microtubules (three independent experiments) the rate was 9060 $\pm$ 3240 molecules of P_i per microtubule per min.

Tubulin Isotype Compositions of Tubulin in High Speed HeLa Cell Extracts and Purified HeLa Cell Tubulin—The foregoing data demonstrate that highly purified tubulin from HeLa cells and from bovine brain polymerize into microtubules that have remarkably different dynamic properties. One possible explanation for the differences in their dynamics may be because of differences in their isotype compositions. Purified bovine brain tubulin consists of 58% $\alpha\beta_{II}$, 25% $\alpha\beta_{III}$, 14% $\alpha\beta_{IV}$, and only 3% $\alpha\beta_I$ (32). Thus, we analyzed the β-tubulin isotype composition of purified HeLa cell tubulin by Western blot analysis with antibodies specific for β_I, β_{II}, β_{III}, and β_{IV} tubulin (see "Experimental Procedures"). Only the β_I and β_{IV} isotypes were detected in the purified HeLa tubulin preparation (Fig. 6*A*), whereas in contrast, purified bovine brain tubulin contained all four isotypes (Fig. 6*A*) as previously reported (32). Densitometric analysis of the blots suggest that the purified HeLa tubulin consists of ~80% α/β_I tubulin and ~20% α/β_{IV} tubulin.

We also wanted to ensure that the purified HeLa cell β-tubulin isotype composition did not represent a selective enrichment of the two β-tubulin isotypes because of the purification procedure. Thus, we probed the clarified HeLa cell extracts (HSS) with the β-specific antibodies (Fig. 6*B*) and detected the β_I and β_{IV} isotypes as the predominant species. While the β_{III} isotype could be faintly detected on heavily overloaded gels, the data suggest that microtubules in HeLa cells are largely composed of $\alpha\beta_I$ and $\alpha\beta_{IV}$.

DISCUSSION

Slow Dynamic Instability and Treadmilling Behavior of Microtubules Prepared from Purified HeLa Cell Tubulin in Vitro—We have characterized the dynamic instability and treadmilling behaviors at steady state *in vitro* using defined solution conditions of microtubules composed of highly purified HeLa cell tubulin. We found that the dynamic instability is remarkably attenuated as compared with the dynamic instability of microtubules made from highly purified MAP-free brain microtubules *in vitro*. Specifically, the total tubulin subunit exchange based upon detectable growth and shortening behavior (the dynamicity) at the plus ends of the HeLa cell microtubules was 0.05 μm/min, a value that is 96% lower than the dynamicity of bovine brain microtubules under equivalent conditions (Table I). During the entire time the HeLa cell microtubules were analyzed (29 microtubules over a total observation time of 172 min), we only observed five transitions from the growing or attenuated state to shortening (catastrophes), which yielded a catastrophe frequency of only 0.02/min. This value is 87% lower than that observed for bovine brain microtubules under similar conditions (Table I). The purified HeLa cell microtubules also exhibited a relatively slow intrinsic steady-state treadmilling rate (~5.3 μm/h). This rate was only ~2-fold faster than that of brain microtubules containing a high content (30%) of stabilizing MAPs (data not shown), which strongly suppress treadmilling (9).

The purified HeLa cell tubulin was devoid of detectable contaminating proteins as determined by Coomassie Blue staining on heavily overloaded SDS-polyacrylamide gels (Fig. 1). It polymerized efficiently in the complete absence of detectable

TABLE I
Dynamic instability parameters of HeLa cell and bovine brain microtubules

Microtubules assembled with HeLa cell tubulin (n = 29) and MAP-free bovine brain tubulin (n = 16) were measured for 172 and 85 min in equivalent dynamic conditions. Values are shown as mean ± S.E.

Parameter	HeLa cell tubulin	Bovine brain (MAP-free) tubulin
Rate (μm/min)		
Growing	0.2 ± 0.02	0.6 ± 0.08
Shortening	7.8 ± 1.3	19.3 ± 2.2
Mean length (μm/event)		
Growing	1.1 ± 0.2	1.3 ± 0.2
Shortening	1.3 ± 0.2	5.0 ± 0.6
Transition frequencies (min^{-1})		
Catastrophe	0.02	0.15
Rescue	5.9	1.6
Percentage of time		
Growing	14.9	67.4
Shortening	0.3	4.5
Attenuated state (paused)	84.8	28.1
Dynamicity (μm/min)	0.05	1.3

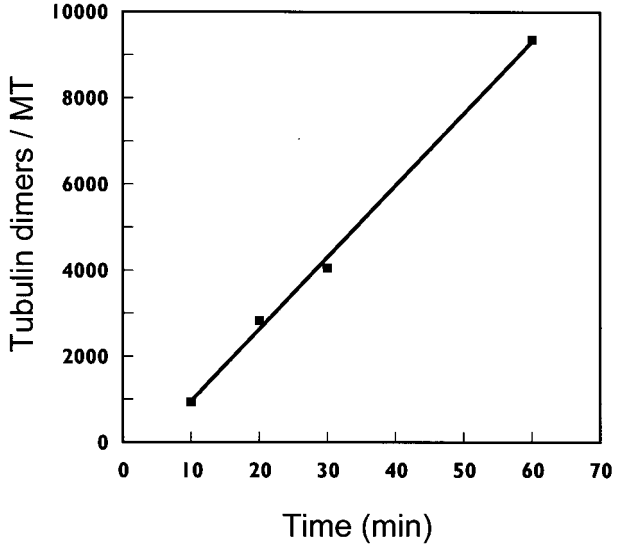

FIG. 4. **Treadmilling rate of HeLa cell microtubules at steady state.** The treadmilling rate was determined by measuring the rate of [^{3}H]GDP incorporation into the steady-state microtubules as described under "Experimental Procedures." The rate of incorporation was 167 tubulin dimers per microtubule per min. For the experiment shown, the microtubule number concentration was 5.94×10^{-10} M. The incorporation rate was calculated by dividing the tubulin concentration (in moles per liter) by the mean microtubule length (μm) × 1690 tubulin dimers per μm.

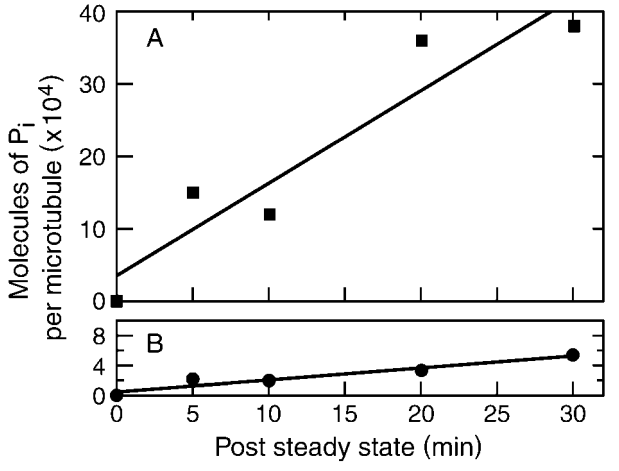

FIG. 5. **Steady-state rate of P_i formation per microtubule for HeLa cell and bovine brain microtubules.** Microtubules were assembled to steady state in PMEM buffer (plus 1 mM GTP) for 30 min after which the evolution of P_i was measured ("Experimental Procedures"). The rate of P_i release per microtubule in the HeLa cell microtubule suspension (*circles*) and the bovine brain microtubule suspension (*squares*) was 1610 and 12,800 molecules of P_i per microtubule per min, respectively. The mean lengths of the microtubules were 14.2 ± 9.5 (μm) for HeLa cell microtubules and 25.9 ± 17.7 (μm) for brain microtubules. The mean microtubule number concentrations were 1.16 (nM) (2.79×10^{-5} M tubulin) and 0.34 (nM) (1.47×10^{-5} M tubulin), for HeLa cell microtubules and bovine brain microtubules, respectively.

MAPs, and it assembled and disassembled efficiently when subjected to cycles of warm assembly-cold disassembly (data not shown). The critical concentration was 0.3 mg/ml (Fig. 2), a concentration that is considerably lower than that of brain tubulin (*e.g.* 1.2 mg/ml) (33). Interestingly, the low critical subunit concentration for HeLa cell microtubules is in the same range as the critical subunit concentrations reported for a number of other nonneural MAP-free tubulins including chick erythrocyte tubulin, sea urchin egg tubulin (*S. purpuratus*), clam egg tubulin, (*Spisula solidissima*), and yeast tubulin (*Saccharomyces cerevisiae*) (18, 34–37). These data indicate that purified HeLa cell microtubules and microtubules from other sources are intrinsically less dynamic than microtubules assembled from neural tubulin.

In accord with their suppressed dynamic instability behavior, the steady-state rate of GTP hydrolysis of the HeLa cell microtubules, which is due primarily to tubulin exchange at the ends of the microtubules, was low. Specifically, the mean rate of GTP hydrolysis was 1390 molecules of GTP per microtubule per min, whereas for brain microtubules, the value under similar conditions was almost 7-fold higher at 9060 molecules of GTP hydrolyzed per min per microtubule (Fig. 5). Because the HeLa cell microtubules did treadmill at a rate of 5.3 μm/h, the treadmilling behavior must have accounted for a fraction (5 times 1690 = 9000 mol of GTP hydrolyzed per h, or ~10%) of the observed steady-state rate of GTP hydrolysis.

The steady-state GTP hydrolysis rate of the HeLa cell microtubules was comparable with that of bovine brain microtubules in the presence of 89% D_2O (805 molecules of GTP per microtubule per min), which reduced the dynamicity of the MAP-free brain microtubules more than 10-fold (14). The steady-state GTP hydrolysis rate of the HeLa cell microtubules was also similar to that of yeast microtubules *in vitro*, which also display highly, attenuated dynamic instability behavior (17, 38).

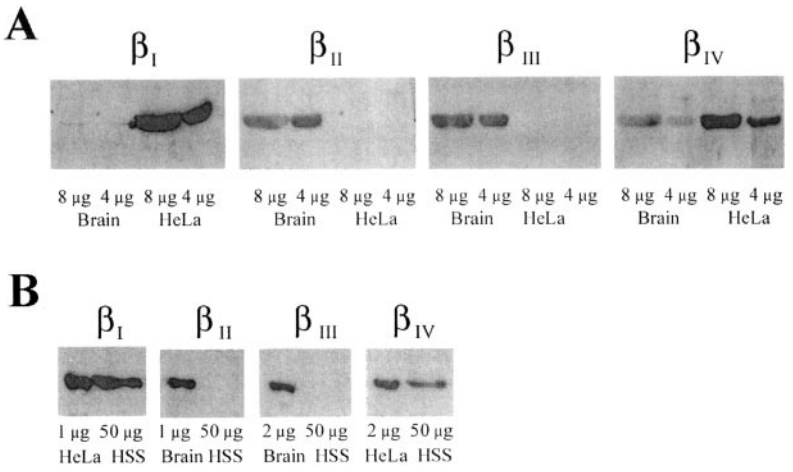

FIG. 6. **Determination of the β-tubulin isotype composition of HeLa cell and bovine brain tubulins by Western blotting with anti-β-tubulin-specific antibodies ("Experimental Procedures").** *A*, β-isotype composition of purified HeLa and brain tubulin. *B*, β-tubulin isotype composition of clarified HeLa cell extracts (HSS). The quantity of protein loaded in each lane is shown. The brain and HeLa cell tubulin blots in *B* are shown as positive controls.

Why Do Purified HeLa Cell Microtubules Display Such Slow Dynamics Compared with Purified Brain Microtubules?—Both the HeLa cell microtubules and the bovine brain microtubules analyzed in this study were made from highly purified tubulins. Furthermore, the dynamic behaviors of the two kinds of microtubules were analyzed under identical experimental conditions. Thus, it is unlikely that the tempered dynamics of the HeLa cell microtubules as compared with that of brain microtubules could have been because of the presence of stabilizing MAPs. One difference between the HeLa cell and bovine brain microtubules that could be responsible for the differences in their dynamics is their β-tubulin isotype compositions. By Western blot analysis we found that the purified HeLa tubulin is composed of ~80% $\alpha\beta_I$ and 20% $\alpha\beta_{IV}$ tubulin (Fig. 6). This isotype composition is significantly different from that of the purified brain microtubules, which consist of a more heterogeneous mixture of β-tubulin isotypes, predominantly 58% $\alpha\beta_{II}$, 25% $\alpha\beta_{III}$, and 14% $\alpha\beta_{IV}$ tubulin and 3% $\alpha\beta_I$ tubulin (32) (Fig. 6). Previous evidence has shown microtubules made from different β-tubulin isotypes have different polymerization properties and exhibit different degrees of dynamic instability behavior (39–42). For example, microtubules composed of $\alpha\beta_{III}$ tubulin are more dynamic than unfractionated neural tubulin or microtubules composed of only $\alpha\beta_{II}$ or $\alpha\beta_{IV}$ (42). In addition, $\alpha\beta_{III}$ tubulin has an ~2-fold higher critical concentration for polymerization than do $\alpha\beta_{II}$ or $\alpha\beta_{IV}$ tubulins (41). Because HeLa cell tubulin consists largely of $\alpha\beta_I$ tubulin, it seems possible that the suppressed dynamics of the HeLa cell microtubules could be because of its high $\alpha\beta_I$ tubulin content.

However, other possibilities besides differences in the isotype compositions also exist. For example, it is well known that tubulins are subjected to a large number of post-translational modifications including tyrosination and detyrosination at the C terminus of α-tubulin, acetylation, glycylation, phosphorylation, and polyglutamylation (reviewed in Ref. 43). Such modifications could well be responsible for, or at least contribute to, the slow dynamics of the HeLa cell microtubules as compared with the brain microtubules.

Regulation of Microtubule Dynamics in Cultured Mammalian Cells—It is curious that in contrast with microtubules made from purified mammalian brain tubulin, microtubules assembled from most other tubulins examined to date exhibit more or less limited dynamic instability behavior *in vitro*. These include microtubules assembled from purified sea urchin egg, chicken erythrocyte, and *S. cerevisiae* tubulins (16–18, 44). It is also curious that dynamics of microtubules made from HeLa cell tubulin or brain tubulin are slower than those of microtubules in living mammalian cells (2, 15). These data may indicate that the tubulin backbone of microtubules, whereas having intrinsic dynamic instability capability, may by itself, display only limited dynamics. If so, this would mean that cellular factors (*e.g.* catastrophe factors) are necessary to create the robust dynamic instability behavior of the highly dynamic microtubules observed *in vivo*. This idea is supported by the work of Simon *et al.* (16) in which the dynamic instability behavior of microtubules assembled in sea urchin extracts was compared with the dynamic instability of microtubules assembled from purified sea urchin tubulin reconstituted in extracts that were devoid of proteins above 30,000 daltons. The microtubules assembled in the filtered extracts exhibited similar dynamic instability behavior to those of microtubules assembled with purified sea urchin tubulin in standard buffer conditions, suggesting that the rapid microtubule dynamics observed in sea urchin extracts were because of proteins larger than 30,000 daltons (16). More recently, identification and characterization of microtubule regulatory factors has fortified this idea (45, 46). In particular, immunodepletion from *Xenopus* extracts of XMAP215, a microtubule-stabilizing factor, or XKCM1, a destabilizing factor, revealed that microtubule dynamics in the extracts is modulated by the antagonistic activities of these factors (45, 46).

It is interesting that microtubules assembled from purified brain tubulin are so much more dynamic than those assembled from HeLa cell tubulin because in neuronal processes, the microtubules are relatively non-dynamic (28, 47), whereas in dividing cells, the microtubules are relatively dynamic (10–13). One possibility is that neuronal microtubules are regulated differently than HeLa cell microtubules. Perhaps in the axons of neuronal cells, the tubulin backbone of the microtubules have intrinsically robust dynamics, but that the dynamics are maintained in a relatively suppressed state by stabilizing MAPs such as MAP2 and tau. However, in the growth cone where robust dynamics are required, the intrinsic dynamic instability behavior is unmasked by inactivation (phosphorylation?) of the stabilizing MAPs. In contrast in HeLa cells, rapid dynamics can be created, as during mitosis, by transiently acting factors that increase the dynamics. Another possibility is that the intrinsic dynamic instability behavior of the tubulin backbone of microtubules from various sources is of little functional consequence, and that the dynamics of the microtubules are determined solely by regulatory factors. If true, isolation and mechanistic characterization of the activities of these factors should lead to a greatly improved understanding of how microtubule dynamics, and thus, dynamics-dependent microtubule function, is controlled in cells.

Acknowledgments—We thank Dr. Richard Luduena (University of Texas Health Science Center, San Antonio) for providing the β-tubulin isotype antibodies, and Dr. Douglas Thrower and Kathy Mitchelson Kamath for critically reading the manuscript.

REFERENCES

1. Hyams, J. S., and Lloyd, C. W. (1994) *Mod. Cell Biol.* **13**, 1–439
2. Desai, A., and Mitchison, T. J. (1997) *Annu. Rev. Cell Dev. Biol.* **13,** 83–117
3. Mitchison, T., and Kirschner, M. (1984) *Nature* **312,** 237–242
4. Horio, T., and Hotani, H. (1986) *Nature* **321,** 605–607
5. Walker, R. A., O'Brien, T. O., Pryer, N. K., Soboeiro, M. F., Voter, W. A., Erickson, H. P., and Salmon, E. D. (1988) *J. Biol. Chem.* **107,** 1437–1448
6. Margolis, R. L., and Wilson L. (1978) *Cell* **13,** 1–8
7. Rodionov, V. L., and Borisy, G. G. (1997) *Science* **275,** 215–218
8. Margolis, R. L., and Wilson, L. (1998) *Bioessays* **20,** 830–836
9. Panda, D., Miller, H. P., and Wilson, L. (1999) *Proc. Natl. Acad. Sci. U. S. A.* **96,** 12459–12464
10. Cassimeris, L., Pryer, N. K., and Salmon, E. D. (1988) *J. Cell Biol.* **107,** 2223–2231
11. Hayden, J. H., Bowser, S. S., and Rieder, C. L. (1990) *J. Cell Biol.* **111,** 1039–1045
12. Verde, F., Labbe, J., Doree, M., and Karsenti, E. (1990) *Nature* **343,** 233–238
13. Rusan, N. M., Fagerstrom, C. J., Yvon, A. C., and Wadsworth, P. (2001) *Mol. Biol.* **12,** 971–980
14. Panda, D., Chakrabarti, G., Hudson, J., Pigg, K., Miller, H. P., Wilson, L., and Himes, R. H. (2000) *Biochemistry* **39,** 5075–5081
15. Cassimeris, L. (1993) *Cell Motil. Cytoskeleton* **26,** 275–281
16. Simon, J. R., Parsons, S. F., and Salmon, E. D. (1992) *Cell Motil. Cytoskeleton* **21,** 1–14
17. Davis, A., Sage, C. R., Wilson, L., and Farrell, K. W. (1993) *Biochemistry* **32,** 8823–8835
18. Gupta, M. L., Bode, C. J., Thrower, D. A., Pearson, C. G., Suprenant, K. A., Bloom, K. S., and Himes, R. H. (2002) *Mol. Biol. Cell* **13,** 2919–2932
19. McNally, F. J. (1996) *Mol. Cell Biol.* **8,** 23–29
20. Anderson, S. S. L. (1999) *BioEssays* **21,** 53–60
21. Cassimeris, L. (1999) *Curr. Opin. Cell Biol.* **11,** 134–141
22. Kinoshita, K., Arnal, I., Desai, A., Drechsel, D. N., and Hyman, A. A. (2001) *Science* **294,** 1340–1343
23. DeLuca, J. D., Newton, C. N., Himes, R. H., Jordan, M. A., and Wilson, L. (2001) *J. Biol. Chem.* **276,** 28014–28021
24. Sackett, D. L. (1995) *Anal. Biochem.* **228,** 343–348
25. Bradford, M. M. (1976) *Anal. Biochem.* **72,** 248–254
26. Detrich, H. W., III, and Wilson, L. (1983) *Biochemistry* **22,** 2453–2462
27. Panda, D., Jordan, M. A., Chu, K. C., and Wilson, L. (1996) *J. Biol. Chem.* **271,** 29807–29812
28. Seitz-Tutter, D., Langford, G. M., and Weiss, D. G. (1988) *Exp. Cell Res.* **178,** 504–511
29. Lanzetta, P. A., Alvarez, L. J., Reinach, P. S., and Candia, O. A. (1979) *Anal. Biochem.* **100,** 95–97
30. Bulinski, J. D., and Borisy, G. G. (1979) *Proc. Natl. Acad. Sci. U. S. A.* **76,** 293–297
31. Ngan, V. K., Bellman, K., Panda, D., Hill, B. T., Jordan, M. A., and Wilson, L. (2000) *Cancer Res.* **60,** 5045–5051
32. Banerjee, A., Roach, M. C., Wall, K. A., Lopata, M. A., Cleveland, D. W., and Luduena, R. F (1988) *J. Biol. Chem.* **263,** 3029–3034
33. Herzog, W., and Weber, K. (1977) *Proc. Natl. Acad. Sci. U. S. A.* **74,** 1860–1864
34. Murphy, D. B., and Wallis, K. T. (1983) *J. Biol. Chem.* **258,** 8357–8364
35. Suprenant, K. A., and Rebhun, L. I. (1983) *J. Biol. Chem.* **258,** 4518–4525
36. Detrich, H. W., III, Jordan, M. A., Wilson, L., and Williams, R. C., Jr. (1985) *J. Biol. Chem.* **260,** 9479–9490
37. Suprenant, K. A., and Rebhun, L. I. (1984) *J. Cell Biol.* **98,** 253–266
38. Dougherty, C., Himes, R. H., Wilson, L., and Farrell, K. W. (1998) *Biochemistry* **37,** 10861–10865
39. Banerjee, A., Roach, M. C., Trcka, P., and Luduena, R. F. (1990) *J. Biol. Chem.* **265,** 1794–1799
40. Banerjee, A., Roach, M. C., Trcka, P., and Luduena, R. F. (1992) *J. Biol. Chem.* **267,** 5625–5630
41. Lu, Q., and Luduena, R. F. (1994) *J. Biol. Chem.* **269,** 2041–2047
42. Panda, D., Miller, H. P., Banerjee, A., Luduena, R. F., and Wilson, L. (1994) *Proc. Natl. Acad. Sci. U. S. A.* **91,** 11358–11362
43. Luduena, R. F. (1998) *Int. Rev. Cytol.* **178,** 207–275
44. Trinczek, B., Marx, A., Mandelkow, E. M., Murphy, D. B., and Mandelkow, E. (1993) *Mol. Biol. Cell* **4,** 323–335
45. Tournebize, R., Popov, A., Kinoshita, K., Ashford, A. J., Rybina, S., Pozniakovsky, A., Mayer, T. U., Walczak, C. E., Karsenti, E., and Hyman, A. A. (2000) *Nat. Cell Biol.* **2,** 13–19
46. Heald, R. (2000) *Nat. Cell Biol.* **2,** E11-E12
47. Okabe, S., and Hirokawa, N. (1988) *J. Cell Biol.* **107,** 651–664

Intrinsically Slow Dynamic Instability of HeLa Cell Microtubules *in Vitro*

Cori N. Newton, Jennifer G. DeLuca, Richard H. Himes, Herbert P. Miller, Mary Ann Jordan and Leslie Wilson

J. Biol. Chem. 2002, 277:42456-42462.
doi: 10.1074/jbc.M207134200 originally published online August 30, 2002
